IEEE Access
Multidisciplinary | Rapid Review | Open Access Journal

Received August 26, 2019, accepted September 7, 2019, date of publication September 17, 2019,
date of current version September 30, 2019.

Digital Object Identifier 10.1109/ACCESS.2019.2941959

Dynamic Bayesian Network Approach to Evaluate Vehicle Driving Risk Based on On-Road Experiment Driving Data

YANLI MA[1], SHOUMING QI[1,2], LUYANG FAN[1], WEIXIN LU[3], CHING-YAO CHAN[2], AND YAPING ZHANG[1]

[1]School of Transportation Science and Engineering, Harbin Institute of Technology, Harbin 150090, China
[2]California PATH, University of California at Berkeley, Berkeley, CA 94804, USA
[3]School of Electronics Engineering and Computer Science, Peking University, Beijing 100871, China

Corresponding author: Yanli Ma (mayanli@hit.edu.cn)

This work was supported in part by the National Key Research and Development Program of China under Grant 2017YFC0803901, in part by the Heilongjiang Highway Survey and Design Institute Project under Grant 2018006, in part by the National Natural Science Foundation of China under Grant 51108136, and in part by the China Scholarship Council Scholarship under Grant 201806120277.

ABSTRACT In this work, we utilize a dynamic Bayesian network for an inferential analysis of driving-related risks based on our assessment of real-world driving data. On-road driving tests are carried out to gather and analyze data to identify different evaluation indicators of driving-related risks. These indicators include the distance between vehicles, acceleration, steering entropy, visual distraction duration, visual glance speed, and blink frequency. Moreover, these indicators are processed to build a driving-related risk evaluation model based on the dynamic Bayesian network. The validity of this model is further tested by experimental data. The results show that this model can achieve a reasonable quantitative evaluation of driving-related risks. Vehicle operation-related risks can be further divided into four levels of safety, namely, levels I to IV. The lowest risk is observed at level I, whereas level IV has the highest risk. Among the indicators for risk evaluation, the distance between vehicles is the most sensitive control indicator of vehicle operation-related risks. The research findings provide various methodologies that could be utilized for evaluation and early warning of driving-related risks. Thus, a theoretical foundation to seek solutions for the safety of advanced driving assistance system is formed.

INDEX TERMS On-road vehicle driving, human factors, driving risk analysis, data analysis, dynamic Bayesian network, road transportation, quantitative evaluation, sensitive control indicator.

I. INTRODUCTION

Road traffic crashes are the ninth leading cause of death, which account for 2.2% of all recorded deaths globally [1]. The number of road traffic-related deaths continues to rise, reaching 1.35 million in 2016 [2]. Meanwhile, China's vehicle ownership and traffic accidents also increase annually. In 2016, China's vehicle ownership reached 300 million, and the number of traffic fatalities was approximately 63,000 (The number is much higher, per this report [3]). Therefore, monitoring the running status of vehicles can effectively improve road traffic safety. The Advanced Driver Assistance System (ADAS) is a vehicle intelligence system that provides operational support for drivers. The existing ADAS mainly works in the hedging phase. If the abnormal state of the vehicle is found at an early stage by the ADAS, a warning can be given in advance to allow the driver sufficient reaction and operation time. Thus, traffic accidents can potentially be avoided or mitigated.

Guo and Fang [4] have found that the driving-related risks of a driver are correlated to his or her accident rate and personality traits. In addition, Simon-Morton *et al.* [5] have observed that a driver's inadequate driving experience and the performance of a secondary task while driving contribute to the risk of vehicle collision. Rosey and Auberlet [6] has reported that vehicle lateral movement is closely related to the state of drivers. For instance, driver's fatigue leads to frequent lane changes. Bargman *et al.* [7] has compared the impact of performing secondary tasks on traffic safety while driving versus eye glance behavior during pursuit. Between the

The associate editor coordinating the review of this manuscript and approving it for publication was Alberto Cano.

two, eye glance behavior has been found to have a greater impact. In addition, Lethaus and Rataj [8] has suggested that eye movements occur earlier than the maneuvers performed by drivers, thus making driving behaviors predictable. Ma *et al.* [9] has also considered the indicators of visual variation duration while driving, such as adjusting the speed, acceleration, lateral displacement, steering wheel rotation speed, and lateral position of the vehicle. The evaluation of distraction risks was conducted based on an approach by support vector machine (SVM). Kircher and Ahlstrom [10] has introduced the driving behavior indicators observed using an eye-tracking algorithm, which aid in improving the accuracy of driving-related risk evaluation. Meanwhile, Xu *et al.* [11] has analyzed the correlation between traffic flow and risks, assessing driving-related risks under different traffic flows. Gershon *et al.* [12] has studied the collected driving data of various young people and has analyzed the interactions between the risk factors of driving and other significant factors.

Among the methods of driving-related risks evaluation, Ng and Hung [13] has applied clustering analysis and regression analysis to evaluate road accident risks. Using vehicle trajectory data, Li and Lu [14] has built a rear-end collision risk model. In addition, Xu *et al.* [15] has comprehensively utilized the theories of gray clustering, fuzzy consistency, and analytic hierarchy process to propose a new systemic approach to road safety evaluation. Meanwhile, Xiong *et al.* [16] has described a prediction algorithm for driving-related risks based on the Markov chain. Wang *et al.* [17] has presented the concept of driving-related risks, which has later been applied to various complex driving scenarios. Cheol *et al.* [18] has used the Bayesian network to develop a warning system for traffic emergencies, which demonstrates the power of the Bayesian network in probability analysis.

In addition, other traditional techniques should also be considered, such as matched case-control logistic regression [19], [20], artificial intelligence models [21], [22], and Bayesian logistic regression [23]. The existing evaluation methodologies have mainly addressed the status of macroscopic traffic operations with efforts to focus on road safety risk and accident risk evaluations. Certain scholars have dedicated their research to on-road driving studies under different road conditions and certain deterministic driving tasks[24]–[26]. Among the identified influence factors of risk are drivers' individual characteristics, eye movement behavior, glance behavior, traffic flow, vehicle maneuver behavior, and operation status. However, the interactions among the influence factors of driving-related risks tend to be neglected.

The Bayesian network is built upon the interactions between variables, and it obtains result distribution by parameter learning and probabilistic reasoning. So far, the Bayesian network has been successfully applied to the risk analysis of aviation system reliability in search and rescue [27] and to the environmental evaluation for operators in the nuclear industry [28], [29]. Wang has applied dynamic Bayesian networks to real-time collision risk assessment of urban expressways [30]. In addition, Guo has studied semi-parametric Bayesian models for evaluating time-variant driving-related risk factors and has used a case-crossover approach to evaluate driver-behavior risks [31].

The assessment of vehicle operating risk is the basis and premise of safety assistance. Appropriate safety assistance can only be carried out after the vehicle risk is correctly assessed. Research on the methods of vehicle safety estimation is also of great significance for improving the core competencies of intelligent transportation vehicles as well as improving the performance of ADAS. In this study, we have applied the dynamic Bayesian network (DBN) to the evaluation of driving-related risks. Data relevant to driving-related risk indicators have been collected in an on-road driving setting. Then, these indicators are utilized to construct a driving-related risk evaluation model based on the Bayesian network. The procedures described in this study for driving-related risk evaluation lay the basis for early assessment and prewarning of driving-related risks. The main research ideas are illustrated in Figure 1.

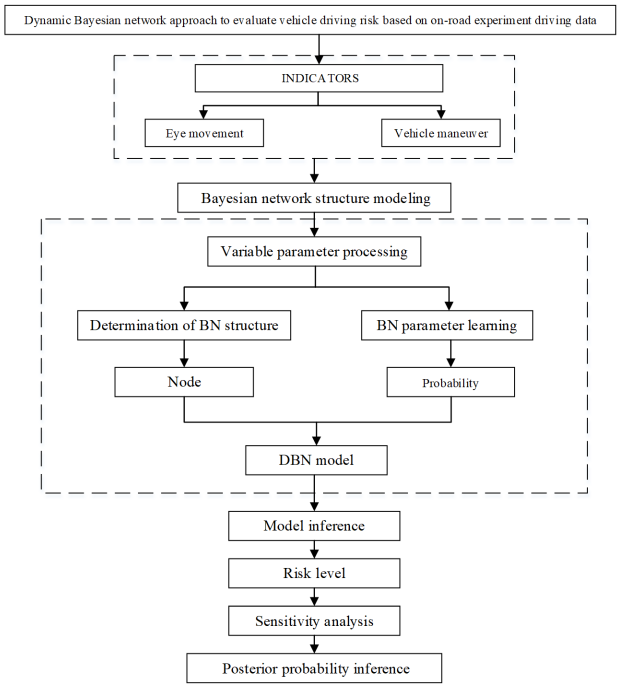

FIGURE 1. Research Framework.

II. EXPERIMENTAL DESIGN

A. PARTICIPANTS

On-road driving tests were performed on 24 participants, and the effective sample is 20 (12 males and 8 females) with different ages (Mean = 34.65, SD = 10.4) and years of driving experience (Mean = 7.5, SD = 7.45). This experiment was organized by the School of Transportation Science and Engineering, Harbin Institute of Technology. Recruitment

details were posted at different schools, taxi companies, and government agencies to recruit suitable drivers. All participants were physically healthy without prior consumption of stimulating and influential substances, such as alcohol and coffee, 24 hours before the test. The basic information description of the participants is shown in Table 1.

TABLE 1. Basic information description of the participants.

Driver Characteristics	All of the participants			
	Mean	Standard Deviation	Number	Percentage
Gender	—	—	20	100%
Male	—	—	12	60%
Female	—	—	8	40%
Age	34.65	10.40	20	100%
≤30	26.2	2.18	10	50%
(30, 40)	35.6	2.15	5	25%
≥40	50.6	4.99	5	25%
Driving age	7.5	7.45	20	100%
<3	1.83	0.37	6	30%
(3, 8)	4.43	1.40	7	35%
≥8	15.43	7.52	7	35%
Driving mileage (10000 km)	6.38	6.91	20	100%
≤3	1.38	0.78	10	50%
(3, 20)	8.68	4.35	8	40%
≥20	22.2	1.7	2	10%
Collision accidents in the past three years	—	—	20	100%
None	—	—	16	80%
Once	—	—	3	15%
More than once	—	—	1	5%
Using mobile phone during driving	—	—	20	100%
Hardly ever	—	—	12	60%
Sometimes	—	—	7	35%
Always	—	—	1	5%

B. APPARATUS

Experimental car was a 2017 Sagitar 1.6T. The experimental equipment included a suite of sensors installed on a passenger car: an eye tracker, acceleration sensors (lateral acceleration and longitudinal acceleration), a steering wheel sensor, a telemeter, a camera, and a driving recorder. The arrangement of the experimental equipment is shown in Figures 2 and 3.

FIGURE 2. Layout of sensor inside the vehicle.

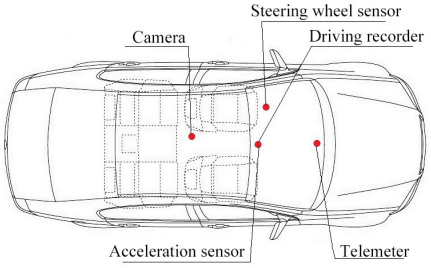

FIGURE 3. Layout of instrument inside the vehicle.

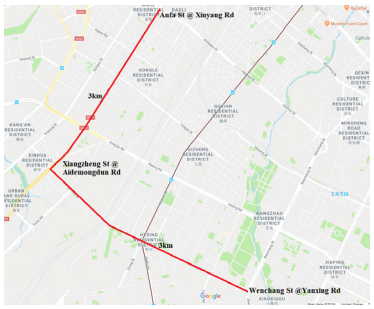

FIGURE 4. Experimental route.

C. EXPERIMENTAL ROUTE

The test was conducted from the intersection of Xinyang Road and Anfa Street to the intersection of Wenchang Street and Yanxing Road in Harbin City, as shown in Figure 4. The road segment from Anfa Street to Xiangzheng Street had an overall length of 3 km on the trunk road. The road segment from Xiangzheng Road to Wenchang Street was the secondary trunk road, which also had an overall length of 3 km. The experiments were conducted during non-peak hours (normally 9:30 am–11:00 am; 2:30 pm–4:00 pm) under favorable weather conditions (sunny, suitable temperature for driving). Road segments with stable traffic flow, ideal road conditions, and little traffic disturbance were chosen for the test.

D. EXPERIMENTAL PROCEDURE

The experimental procedure was as follows:

(1) The participants were asked to fill out a personal information form, and the staff provided them with basic instructions before starting the test.

(2) The participants were instructed to wear significant test instruments (e.g., eye tracker) and adequate time to familiarize themselves with the test vehicle to perform adaptive driving experiments. This process took approximately half an hour.

(3) The driver performed the driving task at the experimental site, whereas the driving video and other data were recorded. The driver then proceeded along the route according to the instructions. If no special or unprecedented situation emerged, then the route could not be changed without authorization. However, depending on the actual road conditions, lane changes could be performed. If the driver perceived that his or her driving

TABLE 2. Main indicator data collected by the tests.

Symbol	Indicator	Unit	Meaning of the parameter	Method of data acquisition
t	Time	s	Start and end time of driving	Driving recorder
VD	Distance between vehicles	m	Distance from the vehicle in front	Laser ranger finder
a	Acceleration	G	Vehicle's acceleration	Acceleration sensor
α	Steering angle	°	Rotation angle of the steering wheel	Steering wheel sensor
BF	Blink frequency	time/s	Blink pattern	Eye tracker
GS	Glance speed	deg/s	Glance behavior	Eye tracker
DT	Visual distraction duration	s	Eye-off-road duration	Eye tracker

was at risk, he or she could bypass the instructions of the guide and perform safe operations. The driving experiment lasted approximately an hour.

(4) Upon completion of the driving task, the staff sorted out and analyzed the driving data. Then, they calibrated the driving risk behaviors. During the calibration process, risky driving behaviors were defined.

III. DATA PROCESSING

In this section, we describe the data processing steps for the on-road driving data. We aimed at generating effective, reliable, and sensitive evaluation indicators of driving-related risks. Consequently, the study found that risky driving could affect driving behavior and reduce the driver's ability to control the vehicle, such as the increase in the number of emergency braking and the increase in the standard deviation of the steering wheel angle. When the driver accepted the execution of different difficulty levels, the vehicle operating parameters, such as vehicle trajectory, speed, and longitudinal and lateral acceleration, changed significantly [32], [33].

Considering the significance of vehicle control and driver behavior to driving-related risks, indicators for vehicle operation and driver's eye movement were collected. The data were used as the judgment variables of vehicle operation risks. The data collected are shown in Table 2.

A. VEHICLE MANEUVER INDICATORS

1) MINIMUM DISTANCE BETWEEN VEHICLES

According to the dynamic formula, two vehicles are located at $X_{\mathrm{i}}$and $X_{\mathrm{i}-1}$ before brake deceleration, and the distance between the vehicles is D_{i}. The front vehicle starts to brake, and the distance in which the *i–1*-th vehicle brakes is $[v_{i-1}(t)]^2/2\alpha_{i-1}(t)$. The distance traveled by the *i*-th vehicle during the reaction time τ is $v_i(t)\tau$, and the distance traveled during the braking process is $[v_i(t)]^2/2\alpha_i(t)$. The formula is as follows:

$$v_i(t)\tau + [v_i(t)]^2 \Big/ 2\alpha_i(t) + d_0 = D_i + [v_{i-1}(t)]^2 \Big/ 2\alpha_{i-1}(t). \tag{1}$$

The distance between two vehicles is

$$D_i = v_i(t)\tau + [v_i(t)]^2 \Big/ 2\alpha_i(t) - [v_{i-1}(t)]^2 \Big/ 2\alpha_{i-1}(t) + d_0. \tag{2}$$

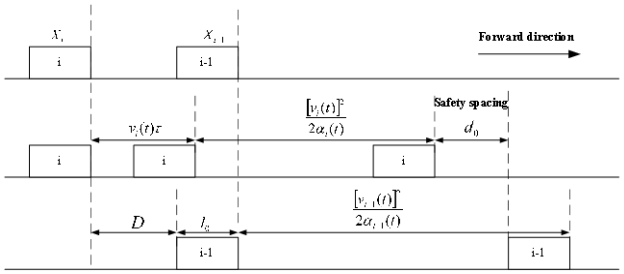

FIGURE 5. Schematic diagram of the vehicle braking process.

TABLE 3. Minimum distance between vehicles under different speeds.

Speed (km/h)	10	20	30	40	50	60	70	80
Minimum distance (m)	5.78	8.56	11.34	14.11	16.89	19.67	21.44	25.22

The two vehicles are assumed to have the same speed and the same latency for the braking to take effect. The minimum distance between the vehicles is shown in Formula (3). The vehicle braking process is shown in Figure 5.

$$D_{\min} = v_i(t)\tau + d_0, \tag{3}$$

where v_i is the driving speed of the *i*-th vehicle before braking begins; τ is the sum of driver's reaction time and latency for the braking to take effect; d_0 is the minimum distance between vehicles after the vehicle has completely stopped.

Assuming that the driver's response time is 0.8 s, the latency for the braking to take effect is 0.2 s, and the d_0 is 3 m. The minimum distances between the two vehicles under different speeds are shown in Table 3.

The ratio of the minimum distance to the actual distance between the two vehicles during driving $\xi(t) = D_{\min}/D(t)$ is used to assess drivers' performance in controlling the distance between the vehicles. This indicator is one way of measuring driving-related risks.

2) ACCELERATION

The temporal variation characteristics of acceleration during on-road driving are shown in Figure 6. The acceleration percentile of the vehicle is shown in Table 4.

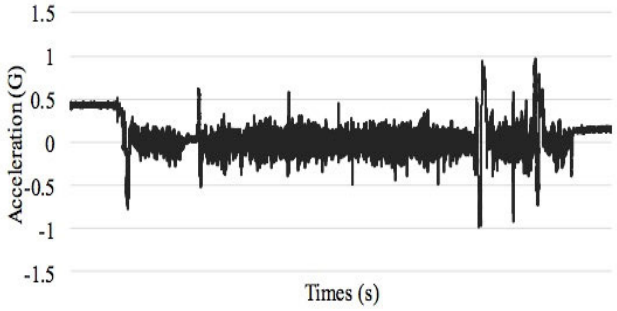

FIGURE 6. Temporal variations of acceleration during driving.

TABLE 4. Acceleration percentile.

Percentile (%)	Acceleration (m/s^2)	Percentile (%)	Acceleration (m/s^2)	Percentile (%)	Acceleration (m/s^2)	Percentile (%)	Acceleration (m/s^2)
5	–1.143 0	30	–0.136 9	60	0.088 0	80	0.292 9
10	–0.647 0	40	–0.050 7	70	0.175 1	90	0.722 6
20	–0.278 5	50	0.022 0	75	0.235 4	95	0.951 3

As shown in Table 4, the probability that the acceleration under -0.6470 m/s^2 or over 0.7226 m/s^2 is relatively small (10%). During the driving process, certain driving-related risks exist if the acceleration falls within this range.

3) STEERING ENTROPY

Steering entropy is a measure of the drivers' ability in operating the steering wheel with smoothness and anticipation of the need to turn the steering wheel. In the relevant literature [34], [35], steering entropy has been proposed to quantify the drivers' steering control capacity.

$$SE = \sum_{i=1}^{9} -p_i \log_9(p_i), \tag{4}$$

where SE is the steering entropy, and p_i is the distribution probability of the prediction errors falling within the error interval.

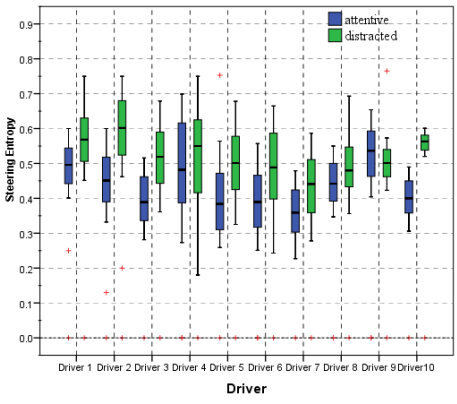

FIGURE 7. Steering entropy for normal and risky driving.

Figure 7 and Table 5 present the steering entropy for normal driving and risky driving from on-road driving tests on 10 drivers under the age of 30 (We studied the driving behavior of young drivers for the time being, and we analyzed data for participants who were under the age of 30.). Except for driver No. 9 (errors resulting from the experimental process), the remaining drivers all showed an apparent increase in the steering entropy (both mean and median.) Thus, the steering entropy was directly proportional to the driving-related risks.

B. EYE MOVEMENT INDICATORS

1) VISUAL DEVIATION DURATION

Visual deviation durations of the drivers are shown in Figure 8, whereas the percentile of the visual deviation duration is shown in Table 6.

As seen from Table 6, the 90th percentile of visual deviation duration was 0.24 s, and the maximum duration was 0.88 s. When the visual deviation duration was less than 1.0 s, the drivers were engaged in collecting the information necessary for the driving task. However, when it was above 1.0 s, the drivers were postulated to exhibit unnecessary eye movements.

2) GLANCE SPEED

The statistics on glance speed during the driving process are shown in Fig. 9. Drivers who came across certain important information showed a dramatic change in the glance speed.

3) BLINK FREQUENCY

Blink frequency reflects the driver's level of brain activity and sensitivity to environmental information. The mean blink frequencies under three statuses of the drivers are shown in Table 7. Evidently, dozing off while driving significantly increased driving-related risks.

IV. MODELING

Representation and inference of Bayesian networks have strict mathematical foundations. Based on probability theory, it examines the statistical regularity of interdependence between multiple variables in objective things, which is very suitable for describing complex systems. The multiple and uncertainty relationship between the representation of events and the situation is one of the most effective theoretical models in the field of uncertain knowledge and reasoning. Therefore, the Bayesian network is used to evaluate and predict vehicle operation risks.

A. BAYESIAN NETWORK STRUCTURE

The risk factors of driving are used as the assessment indicators of driving-related risks. The structure of our proposed Bayesian network model for driving-related risks is shown in Figure 10.

As shown in Figure 10, the hidden nodes are driving-related risk (R), vehicle operation risk (OR), and eye movement-characterized risk (ER), all of which are represented by X_i. Six nodes, namely, steering rotation entropy (SE), acceleration variation rate (a), control index of vehicle

TABLE 5. Descriptive analysis of steering entropy under normal and risky driving.

Category	Items	D1	D2	D3	D4	D5	D6	D7	D8	D9	D10
Normal driving	Mean	0.491	0.450	0.393	0.492	0.397	0.392	0.355	0.441	0.527	0.398
	Median	0.496	0.451	0.388	0.482	0.386	0.390	0.358	0.442	0.537	0.400
	Interquartile range	0.103	0.128	0.127	0.229	0.167	0.151	0.125	0.109	0.131	0.093
	Skewness	–2.077	–1.032	–0.887	–0.535	0.319	–0.648	–1.009	–2.230	–2.214	–2.408
	Kurtosis	12.524	4.246	2.923	0.495	1.426	1.667	2.711	11.198	10.459	12.127
Risky driving	Mean	0.565	0.600	0.510	0.525	0.499	0.491	0.434	0.480	0.499	0.557
	Median	0.568	0.603	0.519	0.551	0.501	0.490	0.441	0.480	0.501	0.563
	Interquartile range	0.124	0.155	0.150	0.208	0.155	0.190	0.154	0.113	0.078	0.043
	Skewness	–1.954	–1.322	–0.920	–0.459	–0.576	–0.580	–0.684	–1.334	–3.904	–2.428
	Kurtosis	12.277	7.290	3.436	0.211	1.931	1.070	1.482	6.735	31.246	9.434

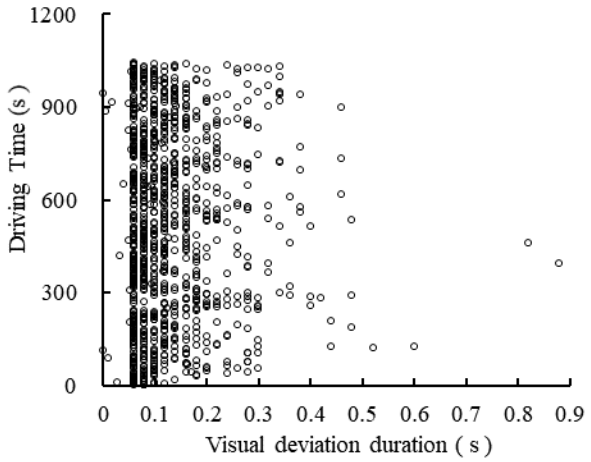

FIGURE 8. Scatter plot of visual deviation duration.

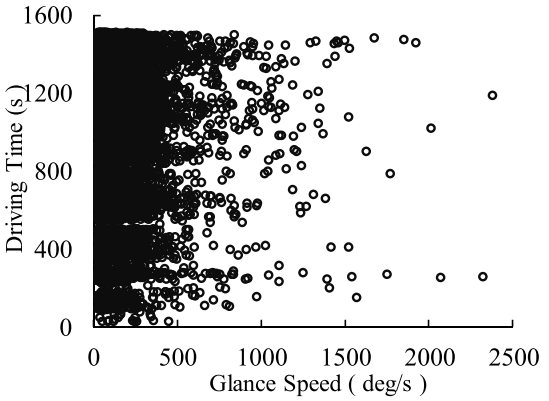

FIGURE 9. Scatter plot of glance speed.

spacing ($\xi(t)$), visual deviation duration (DT), glance speed (GS), and blink frequency (BF), are observational nodes of the status, which is represented by Y_i.

TABLE 6. Percentile of visual deviation duration.

Percentile (%)	20	30	40	50	60	70	80	90
Visual deviation duration (s)	0.06	0.08	0.1	0.1	0.12	0.14	0.18	0.24

The probabilities of hidden nodes R, OR, and ER are given below.

$$P(X_1, X_2, X_3|Y_1, Y_2, \cdots Y_6) = \frac{\prod_i P(X_i|parent(X_i)) \prod_j P(Y_j|parent(Y_j))}{\prod_j P(Y_j)}. \quad (5)$$

From the above,

$$P(X_1|X_2, X_3, Y_1, Y_2, \cdots Y_6) = \frac{P(X_1, X_2, X_2|Y_1, Y_2, \cdots Y_6) \prod_j P(Y_j)}{\prod_m P(X_m) \prod_j P(Y_j|parent(Y_j))}, \quad (6)$$

where $i \in [1, 2], j \in [1, 6], m \in [2, 3]$.

TABLE 7. Mean blink frequencies under three statuses of drivers.

Normal	Dozing	Falling asleep
>0.5 time/s	0.2–0.5 time/s	<0.2 time/s

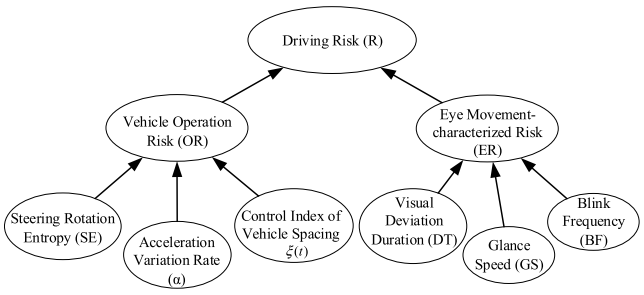

FIGURE 10. BN structure of driving risk.

The status at a specific time point in the static model is chosen for status transfer. Then, in continuous time, the probability of node transfer can be represented by the probability of the nodes at two time points. Let the previous node status be X, then the node status after time T is X'. $P(X'|parent(X'))$ is the conditional probability distribution of node in X'. Let

the transfer probability be β, then

$$\beta = P(X'|X) = \prod_{i=1}^{n} P(X_i'|parent(X_i')). \tag{7}$$

B. DYNAMIC BAYESIAN NETWORK MODEL

The dynamic Bayesian network model of driving-related risks is built upon temporal variation characteristics, as shown in Figure 11.

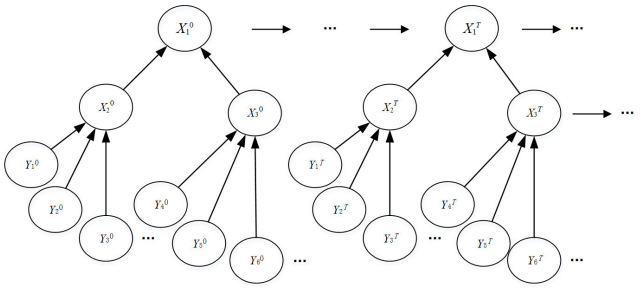

FIGURE 11. DBN for driving risk based on temporal variations.

The model for driving-related risk evaluation can be represented by a collection of static Bayesian networks for each time point within time T. The hidden sequence from the initial 1 to t is represented by X^{t}, whereas the observation sequence is represented by Y^{t}. At time t, the status value of the variable for the i-th hidden node is represented by $x_{\mathrm{i}}^{\mathrm{t}}$, and that of the variable for the$j$-th observational node is represented by $y_{\mathrm{j}}^{\mathrm{t}}$.

With all of the observational nodes given, calculating the probability distribution of hidden nodes corresponding to the existing data is the core of dynamic model inference, (8), as shown at the bottom of this page. According to independence assumption, (9) and (10), as shown at the bottom of this page. From the above formula, the joint probability of risk for time T is derived in (11), as shown at the bottom of this page. Formula (12) can calculate the probability risk at the initial time point, $i \in [0, T]$, $j \in [1, r]$, $k \in [1, 3]$, $n \in [1, T]$, $m \in [2, 3] i \in [0, T]$, $j \in [1, r]$, $k \in [1, 3]$, $n \in [1, T]$, $m \in [2, 3]$.

$$P(x_1^0) = \frac{P(x_1^0, x_1^1, \cdots, x_1^T)}{\prod_n P(x_1^n|parent(x_1^n))} \tag{12}$$

TABLE 8. Occurrence probabilities of vehicle operation indicators under on-road driving.

Vehicle Operation Indicators				
		$\xi(t)$		
Threshold value	(0, 0.8)	(0.8, 0.85)	(0.85, 1)	(1, +∞)
probability	50%	10%	15%	25%
		$\|a\|$		
Threshold value	(0, 0.3)	(0.3, 0.5)	(0.5, 1.3)	(1.3, +∞)
probability	70%	15%	13%	2%
		SE		
Threshold value	(0, 0.5)	(0.5, 0.6)	(0.6, 0.7)	(0.7, +∞)
probability	80%	15%	4.99%	0.01%

TABLE 9. Occurrence probabilities of eye movement-characterized indicators under on-road driving.

Eye movement-characterized indicators				
		DT		
Threshold value	(0, 0.2)	(0.2, 0.4)	(0.4, 1)	(1, +∞)
probability	85%	13.99%	1%	0.01%
		GS		
Threshold value	(0, 440)	(440, 1000)	(1000, 2500)	(2500, +∞)
probability	95%	4.89%	0.1%	0.01%
		BF		
Threshold value	(0, 0.2)	(0.2, 0.5)	(0.5, 1)	(1, +∞)
probability	4%	16%	50%	30%

V. RESULTS AND ANALYSIS

A. MODEL INFERENCE

We selected the threshold based on the percentiles in the statistical analysis of relevant factors. The occurrence probabilities of each observational node during on-road driving are shown in Tables 8 and 9.

$$P(x_1^0, x_2^0, x_3^0, \cdots x_1^T, x_2^T, x_3^T|y_1^0, y_2^0, \cdots, y_6^0, \cdots, y_1^T, y_2^T, \cdots, y_6^T) = \frac{P(x_1^0, x_2^0, x_3^0, \cdots x_1^T, x_2^T, x_3^T, y_1^0, y_2^0, \cdots, y_6^0, \cdots, y_1^T, y_2^T, \cdots, y_6^T)}{\prod_{i,j} P(y_j^i)} \tag{8}$$

$$P(x_1^0, x_2^0, x_3^0, \cdots x_1^T, x_2^T, x_3^T, y_1^0, y_2^0, \cdots, y_6^0, \cdots, y_1^T, y_2^T, \cdots, y_6^T) = \prod_{i,k} P(x_k^i|parent(x_k^i)) \prod_{i,j} P(x_j^i|parent(y_j^i)) \tag{9}$$

$$P(x_1^0, x_2^0, x_3^0, \cdots x_1^T, x_2^T, x_3^T|y_1^0, y_2^0, \cdots, y_6^0, \cdots, y_1^T, y_2^T, \cdots, y_6^T) = \frac{\prod_{i,k} P(x_k^i|parent(x_k^i)) \prod_{i,j} P(y_j^i|parent(y_j^i))}{\prod_{i,j} P(y_j^i)} \tag{10}$$

$$P(x_1^0, x_1^1, \cdots, x_1^T|x_2^0, x_3^0, \cdots, x_2^T, x_3^T, y_1^0, y_2^0, \cdots, y_6^0, \cdots y_1^T, y_2^T, \cdots, y_6^T) = \frac{P(x_1^0, x_2^0, x_3^0, \cdots x_1^T, x_2^T, x_3^T|y_1^0, y_2^0, \cdots, y_6^0, \cdots, y_1^T, y_2^T, \cdots, y_6^T) \prod_{i,j} P(y_j^i)}{\prod_{i,m} P(x_m^i) \prod_{i,j} P(y_j^i|parent(y_j^i))} \tag{11}$$

TABLE 10. Conditional probabilities of inferred risk at each observational node.

Indicator	Threshold value	Probability	Indicator	Threshold value	Probability
$\xi(t)$	(0, 0.8)	5%	DT	(0, 0.2)	5%
	(0.8, 0.85)	10%		(0.2, 0.4)	20%
	(0.85, 1)	25%		(0.4, 1)	25%
	(1, +∞)	60%		(1, +∞)	50%
$\|a\|$	(0, 0.3)	5%	GS	(0, 440)	5%
	(0.3, 0.7)	15%		(440, 1000)	25%
	(0.7, 1.3)	30%		(1000, 2000)	30%
	(1.3, +∞)	50%		(2000, +∞)	40%
SE	(0, 0.5)	2%	BF	(0, 0.2)	40%
	(0.5, 0.6)	8%		(0.2, 0.5)	30%
	(0.6, 0.7)	30%		(0.5, 1)	20%
	(0.7, +∞)	60%		(1, +∞)	10%

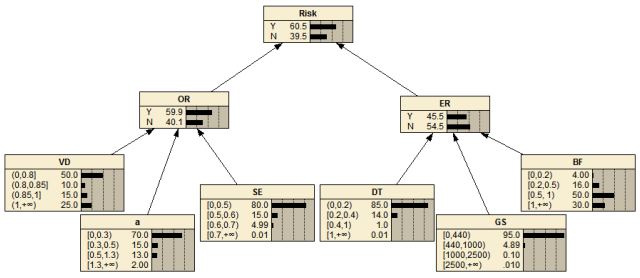

FIGURE 12. Bayesian network model developed by netica.

The conditional probability of the corresponding nodes was calculated based on the structure of the Bayesian network. The conditional probabilities of the inferred risk at each observational node are shown in Table 10.

Netica is a Bayesian network analysis software. It is mainly used for system risk analysis and simulation modeling for system failure. The driving-related risk estimate was obtained from the Bayesian network model using Netica. The conditional probabilities of hidden nodes, vehicle operation risk, eye movement-characterized risk, and the final risk value were calculated. Figure 12 shows the workflow of driving-related risk evaluation. Y indicates risk, whereas N means non-risk. Risk levels were divided based on risk values.

Based on the China National Emergency Response Plan for Public Emergencies, the risk levels were classified into low risk, moderate risk, fairly high risk, and high risk according to the degree of hazard, urgency, and development potential of public emergencies. Depending on the occurrence probability of driving-related risks and the actual operation of the vehicle, the percentage method was used to distribute the probabilities of the four types of risks evenly:

Level **I** (low risk, 0–25%), Level **II** (moderate risk, 25–50%), Level **III**(fairly high risk, 50–75%), and Level **IV** (high risk, 75–100%).

B. SENSITIVITY ANALYSIS

To assess the influence of each observational node, a sensitivity analysis was conducted on each risk. After determining the occurrence probability of risks for each node, the risk factors were ranked in decreasing order of sensitivity, as shown in Table 11.

TABLE 11. Sensitivity analysis.

Node	Mutual info	Percent	Variance of beliefs
Risk	0.968	100	0.2389
OR	0.159	16.400	0.0516
ER	0.117	12.100	0.0369
VD	0.029	3.030	0.0095
α	0.006	0.604	0.0019
SE	0.002	0.197	0.0006
DT	0.001	0.128	0.0004
GS	0.000	0.015	0.0001
BF	0.014	1.400	0.0043

In terms of mutual information (which could reflect the degree of influence between factors), VD, BF, α, SE, DT, and GS declined successively. The degree of influence of each node on a specific risk declined. The distance between vehicles was the most important factor and was the most sensitive among driving-related risks.

To verify whether the data was accurate and whether the analysis function was consistent with the actual situation, the general sensitivity analysis method was utilized. This method is the general algorithm for changing the parameter value to find evident changes. If the factors of the same degree (such as a 10% increase in risk) changed based on the original probability of occurrence, then sensitivity could be judged by observing the influence of each edge probability on the final node.

As shown in the Figure 13, the sensitivity of VD, BF, and α was successively reduced. This conclusion was consistent with the conclusion of Netica sensitivity analysis, proving that the sensitivity analysis made by Netica was reasonable.

C. POSTERIOR PROBABILITY INFERENCE

1) RISK PREDICTION

The evidence variable of a certain situation was input into the Bayesian network, whereas the known state of the evidence variable was used to solve the posterior probability problem of other nodes. In Netica, if the evidence variable was deterministic, setting its state to 100% and updating the probability of the entire network would allow researchers to observe the probability change of the relevant node. As shown in Figure 14, assuming that the driver has poor speed control, the risk of malicious acceleration and deceleration significantly increases from 60.5% to 74.4%.

2) CAUSALITY INFERENCE

Another important application of the Bayesian network is the systematic cause diagnosis. The Bayesian network can perform a two-way inference, which is not only able to calculate the probability of system risk under the joint fault condition

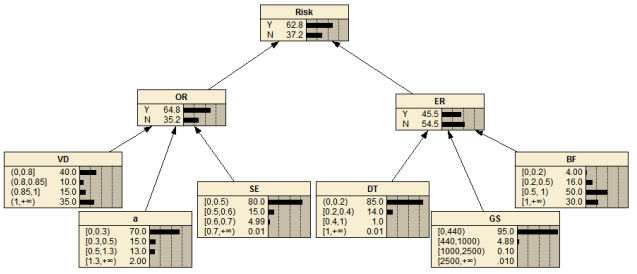

(a) Risk of VD increase 10%

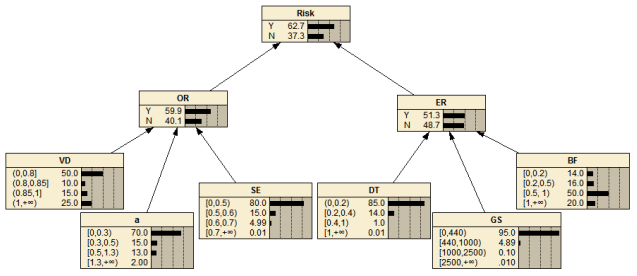

(b) Risk of BF increase 10%

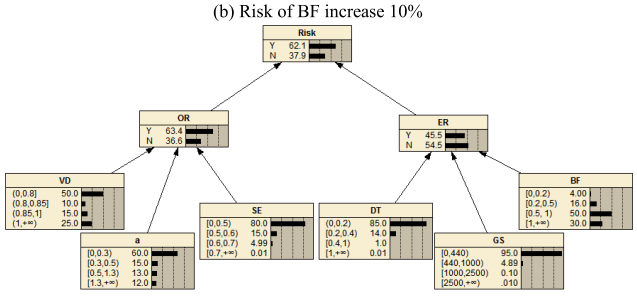

(C) Risk of *a* increase 10%

FIGURE 13. Risk sensitivity analysis.

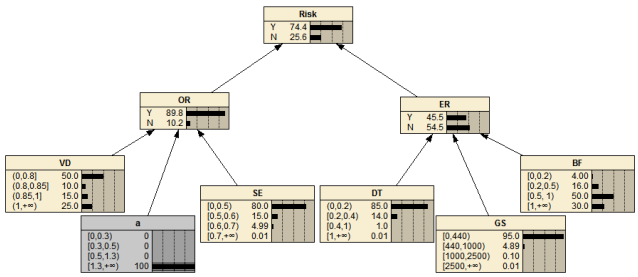

FIGURE 14. Changes in acceleration lead to changes in risk.

of each node but can also calculate the posterior probability of each node under system fault conditions. These conditions can easily find the most likely cause of system failure, thus making an intuitive and convenient analysis.

Assuming that a risk must occur, the state probability was 100%. Figure 15 shows that after the evidence is input through the automatic update function of Netica, the safety of the vehicle operation and the safety of the eye movement representation significantly decreases. The most evident change among the indicators was the observed range of the vehicle distance control index, which was greater than 1 with a significant increase from 25% to 30%. This suggested that, in the absence of other evidence, the most likely cause of the risk was the reduction in vehicle spacing.

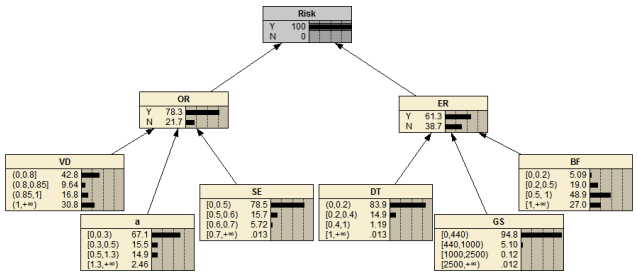

FIGURE 15. Changes in risk status lead to network changes.

VI. DISCUSSIONS AND LIMITATIONS

A. EFFECTIVENESS DETERMINATION OF DBN MODEL

A period of risky driving under on-road driving conditions was compared with that of normal driving, with both periods lasting for 10 s. The results of the indicator values and driving-related risk inference are shown in Tables 12 and 13, respectively.

TABLE 12. Indicator of risk driving in the time period.

Time (s)	Vehicles distance control indicator	Acceleration (m/s^2)	Steering entropy	Visual deviation duration (ms)	Glance speed (Deg/s)	Blink frequency (Time/s)	Risk probability (%)	Risk level
1	0.4698	0.0420	0.0204	0.14	412.27	3	35.1	II
2	0.4713	0.1084	0.4793	0.20	170.05	1	46.4	II
3	0.4745	0.0654	0.6542	0.22	689.67	5	69.1	III
4	0.4762	0.0039	0.5406	0.18	580.33	4	55.7	III
5	0.4762	0.2124	0.1769	0.26	235.88	2	46.4	II
6	0.4828	–0.1347	0.6723	0.18	189.97	2	60.2	III
7	0.4789	0.1435	0.0816	0.18	212.23	3	35.1	II
8	0.4834	0.0283	0.2729	0.06	58.98	1	35.1	II
9	0.4838	–0.1647	0.3910	0.32	40.67	2	46.4	II
10	0.4791	0.0839	0.3663	0.28	595.70	1	46.4	II

TABLE 13. Indicator of normal driving in the time period.

Time (s)	Vehicles distance control indicator	Acceleration (m/s^2)	Steering entropy	Visual deviation duration (ms)	Glance speed (Deg/s)	Blink frequency (Time/s)	Risk probability (%)	Risk level
1	0.2586	0.0670	0.1479	0.10	252.57	3	22.5	I
2	0.2622	0.1084	0.1039	0.08	164.21	1	14.7	I
3	0.2651	0.1654	0.2634	0.20	50.17	3	23.8	I
4	0.2678	0.0039	0.0600	0.16	328.31	2	14.7	I
5	0.2734	0.2124	0.1769	0.18	235.88	4	17.2	I
6	0.2746	–0.1347	0.3473	0.20	189.97	3	28.5	II
7	0.2833	0.1435	0.0816	0.24	433.14	1	37.5	II
8	0.2768	0.0283	0.2729	0.22	58.98	2	30.0	II
9	0.2689	–0.1647	0.3530	0.16	290.67	2	15.3	I
10	0.2732	0.0728	0.1564	0.12	147.07	1	21.4	I

In Figure 16, the risk value for the period of risky driving fluctuates within the range of 35% to 70%. The risk value

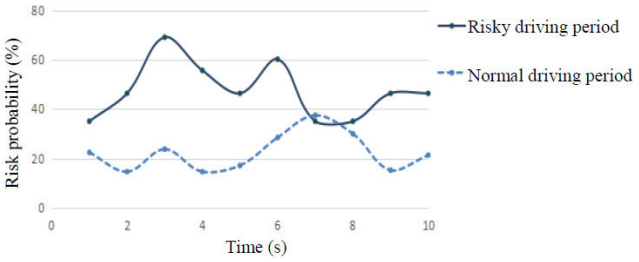

FIGURE 16. Driving risks at different time points.

TABLE 14. 10-fold validation results using ANN.

Fold	Loss	RMSE	MAPE
1	0.0016	0.0369	0.0933
2	0.0019	0.0401	0.0874
3	0.0021	0.0424	0.0879
4	0.0020	0.0446	0.0950
5	0.0036	0.0599	0.1261
6	0.0016	0.0394	0.0867
7	0.0021	0.0456	0.0912
8	0.0016	0.0401	0.0867
9	0.0053	0.0726	0.1436
10	0.0022	0.0464	0.0934
Mean	0.0024	0.0468	0.0991

reaches up to 70% at time point 3, which has been defined as a fairly high risk according to the risk classification criteria. After corrections by the driver's maneuvers, the driving-related risk declined and stabilized at approximately 40%. In contrast, the risk for normal driving fluctuated at approximately 20%, reflecting a low level of risk, whereas the maximum risk for normal driving was below 40%. These results indicated an evident low risk level under normal driving. Thus, the dynamic Bayesian network model proved effective for driving-related risk evaluation, which reflected realistic driving-related risks.

B. METHOD COMPARISON

To verify the performance of the dynamic Bayesian network model, we developed an artificial neural network (ANN) using a fully connected layer assessing the results of the DBN model. The ANN model had two hidden layers, with layer dimensions of 200 and 100. The activation function of the hidden layers was *tanh*, whereas the activation function of the output layer was *Sigmoid*. In addition, the epoch number was 10,000. A ten-fold cross validation was performed on the results of the ANN model. The results of recorded loss, root mean square error (RMSE), and mean absolute percentage error (MAPE) are shown in Table 14. For better comparison, we also used linear regression for the ten-fold cross validation. The results are shown in Table 15.

By comparing Tables 14 and 15, we found that the loss of the ANN model was significantly lower than that of the linear regression model. In addition, the RMSE was also favorable, indicating that the validation of the ANN was

TABLE 15. 10-fold validation results using linear regression.

Fold	Loss	RMSE	MAPE
1	0.0452	0.0301	0.0555
2	0.0717	0.0379	0.0632
3	0.0657	0.362	0.0556
4	0.0674	0.0367	0.059
5	0.0165	0.0182	0.0438
6	0.0149	0.0173	0.0414
7	0.0634	0.0356	0.0602
8	0.0247	0.0222	0.0404
9	0.0478	0.0309	0.0577
10	0.2671	0.0731	0.1959
Mean	0.0685	0.0664	0.06727

better than the linear regression. Given that the hidden layer of the ANN model could express nonlinearity through the activation function *Sigmoid,* we chose the ANN model for deep data learning to examine the Bayesian derivation results further.

The count of true positive rate (TPR) and false positive rate (FPR) of the four risk levels and the plot of the receiver operating characteristic (ROC) curve are shown in Figure 17(a). The separate figures for the four types of risks are shown in Figure 17 (b–e).

Figure 17(a) shows that all the points are concentrated in the upper left portion, wherein the experimental accuracy appears fitting, indicating that the model learning effect is also sound. At the same time, the four types of risks were analyzed. Additionally, the identifications of risks II and III were better, whereas the effect of risk IV was worse. In the future, the Bayesian network could be deduced by adding more risk indicators for a better learning of the model.

C. LIMITATIONS

(1) At present, the parameters determination method of Bayesian network is mainly based on expert systems and parameter learning, which more or less deviates from the actual situation.

(2) The network topology determined based on expert knowledge is relatively simple. The determination of the topology of relatively complex systems and its structural learning are subject to further study.

(3) Given the limitations of test conditions and equipment, the selection factors of variables and prediction models also have limitations. Thus, comprehensive consideration should be added in future research, such as driver's personality, vehicle type, and deviation from the center of the line. At the same time, more samples should be collected for reinforcement learning, which improves the accuracy and precision of the model.

(4) The division of driving risk levels needs to be more objective, and future research should combine the established ANN model to carry out the risk division of clustering.

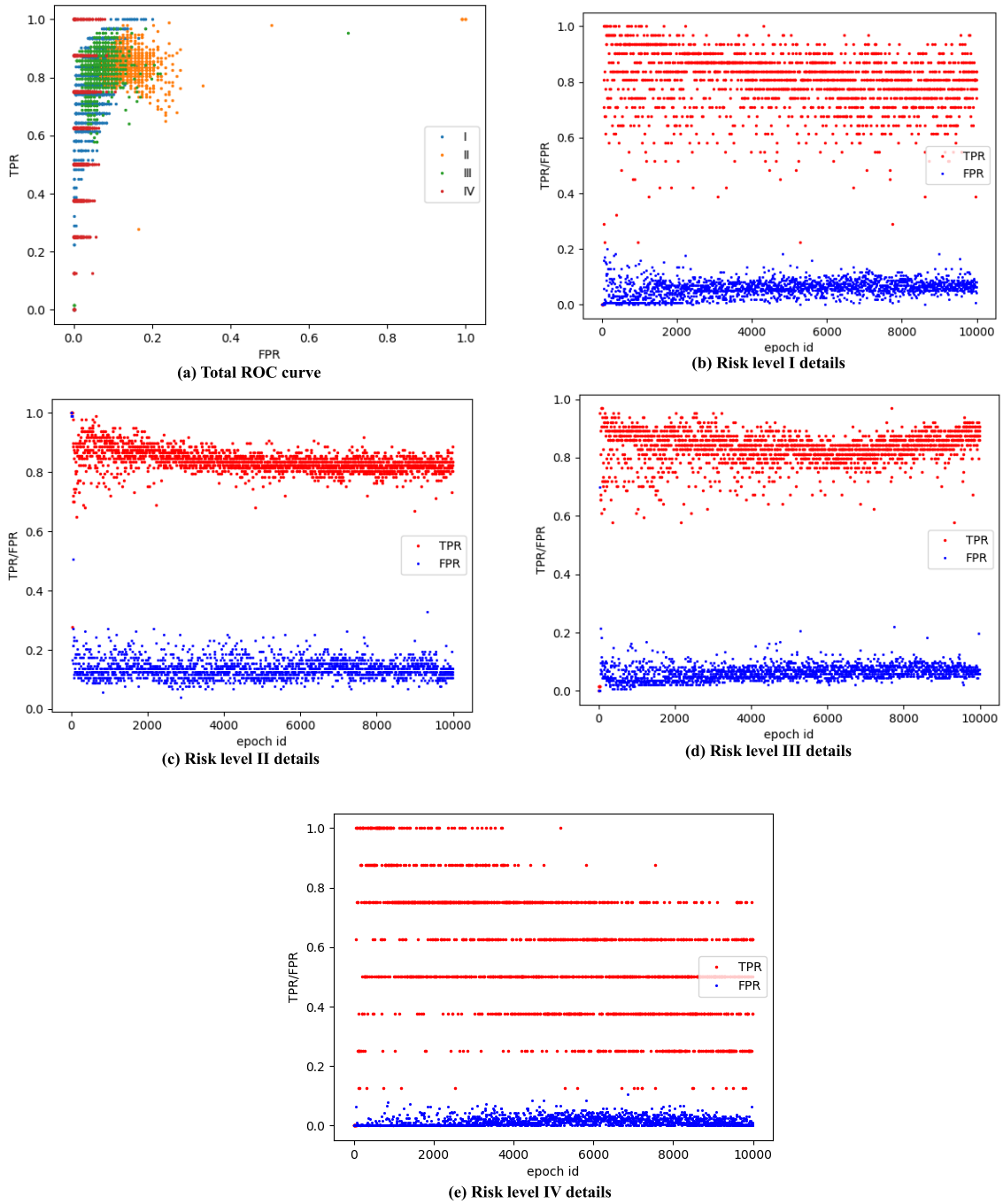

FIGURE 17. ROC curves for four risk states.

VII. CONCLUSION

(1) The on-road driving test was conducted to obtain data on the following indicators of driving-related risks: control indicator distance between vehicles, acceleration, steering entropy, visual deviation duration, glance speed, and blink frequency. The occurrence probability of the driving risks was analyzed based on these indicators. The thresholds of each indicator for each risk level were also determined.

(2) A dynamic Bayesian network model was developed to assess driving-related risks. The results showed that the proposed model could quantitatively describe the driving-related risks under the influence of different dynamic factors. The dynamic Bayesian network model was used to calculate and infer driving-related risks via Netica in a spectrum of safe to unsafe driving at four different risk levels. Sensitivity analysis indicated that the distance between vehicles was most sensitive among the driving-related risks.

(3) The periods of normal and risk driving were compared under on-road driving conditions. The dynamic Bayesian network model was further verified for

its capability in evaluating driving-related risks. Constructing the ANN model to gather the dynamic Bayesian network risk derivation results showed that the learning effect was fitting but was also subject to the selection of indicators and other factors. Alternatively, the prediction of risk levels II and III were more accurate.

ACKNOWLEDGMENT

The authors had the gratitude to the reviewers and appreciated the valuable comments from the doctoral students of Institute of Traffic Engineering and colleagues at UC Berkeley PATH.

REFERENCES

[1] *Global Status Report on Road Safety 2018*. Geneva, Switzerland: World Health Org., 2018.
[2] *Annual Global Road Crash Statistics*. Accessed: 2017. [Online]. Available: https://www.asirt.org/safe-travel/road-safety-facts/
[3] C. Chi-Yuk. *Traffic's Toll: Road Accidents Kill 700 People a Day in China*. South China Morning Post. Accessed: May 24, 2016. [Online]. Available: https://www.scmp.com/news/china/society/article/1952218/traffics-toll-road-accidents-kill-700-people-day-china
[4] F. Guo and Y. Fang, "Individual driver risk assessment using naturalistic driving data," *Accident Anal. Prevention*, vol. 61, no. 6, pp. 3–9, Dec. 2013.
[5] B. G. Simons-Morton, J. P. Ehsani, P. Gershon, S. G. Klauer, and T. A. Dingus, "Teen driving risk and prevention: Naturalistic driving research contributions and challenges," *Safety*, vol. 3, no. 4, p. 29, Dec. 2017.
[6] F. Rosey and J.-M. Auberlet, "Driving simulator configuration impacts drivers' behavior and control performance: An example with studies of a rural intersection," *Transp. Res. F, Traffic Psychol. Behav.*, vol. 27, pp. 99–111, Nov. 2014.
[7] J. Bärgman, V. Lisovskaja, T. Victor, C. Flannagan, and M. Dozza, "How does glance behavior influence crash and injury risk? A 'what-if' counterfactual simulation using crashes and near-crashes from SHRP2," *Transp. Res. F, Traffic Psychol. Behav.*, vol. 35, pp. 152–169, Nov. 2015.
[8] F. Lethaus and J. Rataj, "Do eye movements reflect driving manoeuvres?" *IET Intell. Transp. Syst.*, vol. 1, no. 3, pp. 199–204, Sep. 2007.
[9] Y. L. Ma, G. F. Gu, and Y. E. Gao, "Driver distraction judging model under in-vehicle information system operation based on driving performance," *China J. Highway Transp.*, vol. 29, no. 4, pp. 123–129, 2016.
[10] K. Kircher and C. Ahlstrom, "Predicting visual distraction using driving performance data," *Ann. Adv. Automot. Med.*, vol. 54, pp. 333–342, Jan. 2010.
[11] C. Xu, P. Liu, W. Wang, and Z. Li, "Evaluation of the impacts of traffic states on crash risks on freeways," *Accident Anal. Prevention*, vol. 47, pp. 162–171, Jul. 2012.
[12] P. Gershon, J. Ehsani, C. Zhu, F. O'Brien, S. Klauer, T. Dingus, and B. Simons-Morton, "Vehicle ownership and other predictors of teenagers risky driving behavior: Evidence from a naturalistic driving study," *Accident Anal. Prevention*, vol. 118, pp. 96–101, Sep. 2018.
[13] K.-S. Ng, W.-T. Hung, and W.-G. Wong, "An algorithm for assessing the risk of traffic accident," *J. Saf. Res.*, vol. 33, no. 3, pp. 387–410, Oct. 2002.
[14] Y. Li and J. Lu, "Analysis of rear-end risk for driver using vehicle trajectory data?" *J. Southeast Univ. (English Ed.)*, vol. 33, no. 2, pp. 236–240, 2017. doi: 10.3969/j.issn.1003-7985.2017.02.018.
[15] H.-G. Xu, Z.-H. Liu, and C. Wang, "Road safety level evaluation based on grey fixed weight clustering model and factors analysis," *J. Traffic Transp. Eng.*, vol. 7, no. 2, pp. 94–98, 2007.
[16] X. Xiong, L. Chen, and J. Liang, "Vehicle driving risk prediction based on Markov chain model," *Discrete Dyn. Nature Soc.*, vol. 2018, Jan. 2018, Art. no. 4954621. doi: 10.1155/2018/4954621.
[17] J. Wang, J. Wu, and Y. Li, "Concept, principle and modeling of driving risk field based on driver-vehicle-road interaction," *China J. Highway Transp.*, vol. 29, no. 1, pp. 105–114, 2016.
[18] C. Oh, J.-S. Oh, and S. G. Ritchie, "Real-time hazardous traffic condition warning system: Framework and evaluation," *IEEE Trans. Intell. Transp. Syst.*, vol. 6, no. 3, pp. 265–272, Sep. 2005.
[19] M. Abdel-Aty, N. Uddin, and A. Pande, "Split models for predicting multivehicle crashes during high-speed and low-speed operating conditions on freeways," *Transp. Res. Rec.*, vol. 1908, no. 1, pp. 51–58, 2005. doi: 10.1177/0361198105190800107.
[20] M. M. Ahmed, M. Abdel-Aty, and R. Yu, "Bayesian updating approach for real-time safety evaluation with automatic vehicle identification data," *Transp. Res. Rec.*, vol. 2208, no. 1, pp. 60–67, 2012. doi: 10.3141/2280-07.
[21] R. Yu and M. Abdel-Aty, "Utilizing support vector machine in real-time crash risk evaluation," *Accident Anal. Prevention*, vol. 51, pp. 252–259, Mar. 2013.
[22] J. Sun, J. Sun, and P. Chen, "Use of support vector machine models for real-time prediction of crash risk on urban expressways," *Transp. Res. Rec.*, vol. 2432, no. 1, pp. 91–98, 2014. doi: 10.3141/2432-11.
[23] C. Xu, W. Wang, P. Liu, R. Guo, and Z. Li, "Using the Bayesian updating approach to improve the spatial and temporal transferability of real-time crash risk prediction models," *Transp. Res. C, Emerg. Technol.*, vol. 38, pp. 167–176, Jan. 2014.
[24] H. Raha, T. S. Peter, and J. G. Timothy, "Driver speed selection and crash risk: Insights from the naturalistic driving study," *J. Saf. Res.*, vol. 63, pp. 187–194, Dec. 2017.
[25] K. Tuomo and M. Jakke, "Naturalistic study on the usage of smartphone applications among Finnish drivers," *Accident Anal. Prevention*, vol. 115, pp. 53–61, Jun. 2018.
[26] P. Blazej, S. P. Guillaume, and D. Patricia, "Evaluating individual risk proneness with vehicle dynamics and self-report data–toward the efficient detection of At-risk drivers," *Accident Anal. Prevention*, vol. 123, pp. 140–149, Feb. 2019.
[27] J. T. Luxhoj, "Probabilistic causal analysis for system safety risk assessments in commercial air transport," in *Proc. Workshop Investigating Reporting Incidents Accidents*, Williamsburg, VA, USA, 2003, pp. 17–38.
[28] L. Norrington, J. Quigley, A. Russell, and R. Van der Meer, "Modelling the reliability of search and rescue operations with Bayesian Belief Networks," *Rel. Eng. Syst. Saf.*, vol. 93, no. 7, pp. 940–949, Jul. 2008.
[29] M. C. Kim and P. H. Seong, "An analytic model for situation assessment of nuclear power plant operators based on Bayesian inference," *Rel. Eng. Syst. Saf.*, vol. 91, no. 13, pp. 270–282, Mar. 2006.
[30] K. Yang, X. Wang, and R. Yu, "A Bayesian dynamic updating approach for urban expressway real-time crash risk evaluation," *Transp. Res. C, Emerg. Technol.*, vol. 96, pp. 192–207, Nov. 2018.
[31] F. Guo, I. Kim, and S. G. Klauer, "Semiparametric Bayesian models for evaluating time-variant driving risk factors using naturalistic driving data and case-crossover approach," *Statist. Med.*, vol. 38, no. 2, pp. 160–174, Jan. 2019. doi: 10.1002/sim.7574.
[32] S. Tokuda, G. Obinata, E. Palmer, and A. Chaparro, "Estimation of mental workload using saccadic eye movements in a free-viewing task," in *Proc. Annu. Int. Conf. IEEE Eng. Med. Biol. Soc.*, Aug./Sep. 2011, pp. 4523–4529.
[33] N. Merat, A. H. Jamson, F. C. H. Lai, and O. Carsten, "Highly automated driving, secondary task performance, and driver state," *Hum. Factors*, vol. 54, no. 5, pp. 762–771, 2012.
[34] M. Pavelka and P. Vysoký, "Indication of driver fatigue with help of steering wheel movement," in *Proc. 7th WSEAS Int. Conf. Autom. Control, Modeling Simul.*, May 2005, pp. 548–551.
[35] N. Okihiko, F. Tohru, and N. Tomokazu, "Development of a steering entropy method for evaluating driver workload," SAE Tech. Rep. 01–1999-0892, 1999.

YANLI MA received the B.S. and M.S. degrees in traffic engineering and the Ph.D. degree in road and railway engineering from the Harbin Institute of Technology, Harbin, China, in 1997, 2002, and 2007, respectively.

From 1997 to 2007, she was a Research Assistant with the School of Transportation Science and Engineering, Harbin Institute of Technology. She has been an Associate Professor, since 2007. Her research interests include road traffic safety theory and technology, driver behavior and human–computer interaction, driving distraction characteristic, and secondary tasks. She is a member of the American Society of Civil Engineering and Easter Asia Society for Transportation Studies.

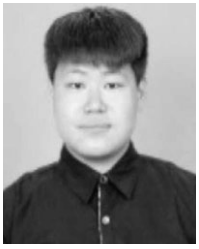

SHOUMING QI received the B.S. degree in civil engineering from Ludong University, Yantai, China, in 2013, and the master's degree in transportation engineering from the Kunming University of Science and Technology, Kunming, China, in 2016. He is currently pursuing the Ph.D. degree in traffic engineering with the Harbin Institute of Technology, Harbin, China.

He has been a Visiting Scholar with UC Berkeley PATH, since September 2018. His research interests include human-machine driving in autonomous vehicle, machine learning, characteristics of driver's performance, characteristics of driving distraction, and traffic congestion problems. He was a recipient of the China National Master Scholarship, in 2015.

LUYANG FAN received the B.S. and master's degrees in transportation engineering from the Harbin Institute of Technology, Harbin, China, in 2016 and 2018, respectively. She is currently an Engineer in Chengdu. Her main research interest includes driver behavior and traffic safety.

WEIXIN LU is currently pursuing the bachelor's degree in computer science with the School of Electronic Engineering and Computer Science, Peking University, Beijing, China. His research interests include graph database, graph embedding, and reinforcement learning.

CHING-YAO CHAN received the Ph.D. degree in mechanical engineering from the University of California at Berkeley (UC Berkeley), Berkeley, CA, USA, in 1988.

He is currently a Research Engineer with the California Partners for Advanced Transportation Technology (PATH), UC Berkeley, where he joined, in 1994. Since 2009, he has been a Program Leader with the Transportation Safety Research Area, California PATH. His research interests include the development of driver-assistance systems, evaluation of sensing, wireless communication technologies to vehicular safety systems, and highway network safety assessment. He possesses in-depth knowledge in specialty areas of safety systems and technology use for transportation applications.

YAPING ZHANG received the B.S. degree in photogrammetry and remote sensing from Wuhan University, China, in 1988, the M.S. degree in road and railway engineering from Hunan University, China, in 1999, and the Ph.D. degree in road and railway engineering from the Harbin Institute of Technology, China, in 2005.

From 1988 to 2000, he was a Lecturer with the Changsha Transportation College. From 2001 to 2004, he was an Associate Researcher with the Changsha University of Science and Technology. He is currently a Professor with the Harbin Institute of Technology, where he joined, in 2005. His research interests include traffic design and planning, transportation safety, traffic simulation, logistic engineering, and 3S technology.